Journal of Solid State Chemistry 183 (2010) 444–450

Contents lists available at ScienceDirect

Journal of Solid State Chemistry

journal homepage: www.elsevier.com/locate/jssc

Synthesis, structure and theoretical studies of a new ternary non-centrosymmetric β-$LaGaS_3$

Peng Li [a,b], Long-Hua Li [a,b], Ling Chen [a], Li-Ming Wu [a,*]

[a] State Key Laboratory of Structural Chemistry, Fujian Institute of Research on the Structure of Matter, Chinese Academy of Sciences Fuzhou, Fujian 350002, PR China
[b] Graduate School of Chinese Academy of Sciences, Beijing 100039, PR China

ARTICLE INFO

Article history:
Received 2 September 2009
Received in revised form
22 November 2009
Accepted 29 November 2009
Available online 5 December 2009

Keywords:
Lanthanum gallium sulfide
Electronic structure
Band gap
Optical property
NLO

ABSTRACT

New ternary β-$LaGaS_3$ has been synthesized from the stoichiometric mixture of elements by a conventional solid-state reaction at 1100 °C and annealed at 820 °C. This compound represents a new structure type that crystallizes in a non-centrosymmetric orthorhombic space group $Pna2_1$ (No.33) with a=10.405(1) Å, b=21.984(2) Å, c=6.0565(5) Å, and Z=12, and features the wavy GaS_4 tetrahedron chains that are separated by La^{3+} cations. Detailed structural differences between the title compound and its isomer, monoclinic α-$LaGaS_3$, are discussed. With the aid of WIEN2k package, the absorption spectra and electronic structures as well as the refractive indexes, absorption coefficients and reflectivities of two types of $LaGaS_3$ have been calculated. The calculated band gap and the absorption edge of β-$LaGaS_3$ agree well with the experimental measurements. And a weak NLO response of β-$LaGaS_3$ has been detected.

1. Introduction

The generation of lasers with high power tunable in the range of 3–20 μm, especially in the regions of 3–5 and 8–14 μm that are known of the two atmospheric transparent windows, has become the focus of the infrared (IR) laser research [1–2]. The nonlinear optical (NLO) materials can simply convert the frequency of an achieved laser into a new one, and new chalcogenide-based NLO materials have been continuously found [3–6].

Ternary chalcogenides with the general formula ABC_2 (A=Li, Na, Cu, Ag; B=Al, Ga, In; C=S, Se, Te) [7] have shown a wide spectrum of potential optoelectronic applications, such as NLO materials, solar energy converters, light emitting diodes (LED) and detectors. Usually, these compounds belong to two crystallographic categories according to the identity of the "A" cation. If A represents a noble-metal cation (A=Cu, Ag), the compound adopts chalcopyrite structure (tetragonal $I\bar{4}2d$, point group $\bar{4}2m$); if A means an alkali metal (A=Li, Na), the structure belongs to orthorhombic α-$NaFeO_2$ type (orthorhombic $Pna2_1$, point group $mm2$) [8].

The well known lanthanide-containing chalcogenide glass La–Ga–S (LGS) is a class of NLO material that has a wide IR transmission window. The transmission rate of LGS is of 50% or higher through a 1 mm thickness over a wavelength range of 0.5–10 μm. Owing to its high glass transition temperature, T_g=580 °C, LGS can be utilized in high-temperature applications [9–11]. Furthermore, several reportes have shown that LGS can achieve a high lanthanide (Ln) doping concentration without clustering, because Ln ions can substitute La^{3+} ions in the glass matrix [12]. For example, LGS glass doped with Nd^{3+} has been investigated for its potential applications as a laser material. On the other hand, ternary $Ln/B/C$ (Ln=La–Lu; B=Al, Ga, In; C=S, Se, Te) are less studied. Up to now, only two ternary La/Ga/S compounds are reported: α-$LaGaS_3$ (monoclinic, $P2_1/c$) [13], and hexagonal phase $La_6Ga_{3.33}S_{14}$ ($Ce_6Al_{3.33}S_{14}$ type) [14].

In this paper, we present the synthesis, structure of a new β-type non-centrosymmetric orthorhombic $LaGaS_3$. The structural relationship between isomeric α- and β-$LaGaS_3$ has been presented. The electronic band structures and optical property calculations on both compounds on the basis of WIEN2k have been reported for the first time.

2. Experimental section

2.1. Synthesis

All starting reactants were handled inside an N_2-filled glove box with controlled oxygen and moisture levels below 0.1 ppm. La (99.5% or higher, Huhhot Jinrui Rare Earth Co. Ltd), Ga shot (99.99999%, Sinopharm Chemical Reagent Co., Ltd) and S shot (99.99%, Alfa Aesar) were used as received. The stoichiometric element mixture with an overall weight about 300 mg of La, Ga

* Corresponding author. Fax: +86 591 83704947.
E-mail address: liming_wu@fjirsm.ac.cn (L.-M. Wu).

0022-4596/$ - see front matter © 2009 Elsevier Inc. All rights reserved.
doi:10.1016/j.jssc.2009.11.030

and S (1:1:3 in molar ratio) were weighed and put into a graphite crucible. The loaded crucible was put into a quartz tube, and then flame-sealed under vacuum 10^{-3} Pa. Such a sealed assembly was placed into a temperature controlled tube furnace, held constant at 450 °C for 10 h, then heated to 1100 °C in 20 h and kept for 120 h, subsequently cooled to 820 °C in 2 h and kept for 120 h, and finally cooled to room temperature over 72 h. Single crystals of the light yellow title compound were obtained, and the compound is stable in air over a period of weeks.

2.2. Crystal structure determination

The single crystal diffraction data were collected on a Rigaku SCXmini diffractometer equipped with a graphite-monochromated Mo$K\alpha$ radiation (λ=0.71073 Å) at room temperature. The structure was solved by the direct method and refined on F^2 by full-matrix least-squares methods using the SHELX97 program package [15]. All atoms were refined with anisotropic thermal parameters. The Flack parameter was refined to −0.01(1), indicating the absolute structure is correct. Crystallographic data and details of the collection are presented in Table 1. The positional coordinates and isotropic equivalent thermal parameters are given in Table S1. Selected bond distances are listed in Table 2.

Crystallographic data in CIF format for β-$LaGaS_3$ has been given as Supporting Materials. This data can also be obtained from the Fachinformationszentrum Karlsruhe, 76344 Eggenstein-Leopoldshafen, Germany (fax: +49 7247 808 666; e-mail: crysdata@fiz-karlsruhe. de) on quoting the depository number ICSD 420964.

2.3. X-ray powder diffraction

The X-ray powder diffraction (XRD) patterns were collected on an XPERT-MPD θ–2θ diffractometer with Cu$K\alpha$ radiation (λ=1.5406 Å) at a scanning rate of 5°/min over 2θ ranging from 5° to 85°. The XRD was measured on the as-synthesized powders, which turned out to be a mixture of β-$LaGaS_3$ (roughly 60%) and $La_6Ga_{3.33}S_{14}$ (roughly 40%) (Fig. 1).

Table 1
Crystallographic data and refinement details for β-$LaGaS_3$.

Formula	β-$LaGaS_3$
Fw	304.81
Crystal system	Orthorhombic
Crystal color	Light yellow
Z	12
Space group	$Pna2_1$
a (Å)	10.405(1)
b (Å)	21.984(2)
c (Å)	6.0565(5)
V (Å^3)	1385.3(2)
F(000)	1632
D_c (g cm^{-3})	4.38424
Flack parameter	−0.01(1)
μ (mm^{-1})	16.109
$2\theta_{max}$ (deg)	55.02
GOOF on F^2	1.083
R_1, wR_2 ($I>2\sigma(I)$)[a]	0.0133, 0.0279
R_1, wR_2 (all data)	0.0143, 0.0328

$R_1 = \sum ||F_0|-|F_c|| / \sum |F_0|, wR_2 = [\sum w(F_0^2-F_c^2)^2 / \sum w(F_0^2)^2]^{1/2}$.

Table 2
Selected bond lengths (Å) of β-$LaGaS_3$.

La(1)–S(9)	2.816(1)	La(3)–S(2)	2.944(1)
La(1)–S(9)	2.841(1)	La(3)–S(8)	2.982(1)
La(1)–S(2)	2.948(1)	La(3)–S(5)	2.997(1)
La(1)–S(6)	2.964(1)	La(3)–S(3)	3.013(2)
La(1)–S(7)	2.994(1)	La(3)–S(3)	3.314(2)
La(1)–S(8)	3.028(1)	Ga(1)–S(8)	2.207(1)
La(1)–S(1)	3.137(2)	Ga(1)–S(5)	2.255(1)
La(1)–S(1)	3.260(2)	Ga(1)–S(6)	2.316(1)
La(2)–S(3)	2.896(1)	Ga(1)–S(7)	2.323(1)
La(2)–S(8)	2.971(1)	Ga(2)–S(9)	2.195(2)
La(2)–S(5)	2.986(1)	Ga(2)–S(7)	2.256(1)
La(2)–S(2)	2.987(1)	Ga(2)–S(1)	2.274(1)
La(2)–S(7)	3.051(1)	Ga(2)–S(6)	2.305(1)
La(2)–S(5)	3.057(1)	Ga(3)–S(4)	2.253(1)
La(2)–S(4)	3.064(2)	Ga(3)–S(3)	2.258(1)
La(2)–S(4)	3.261(2)	Ga(3)–S(2)	2.319(2)
La(3)–S(4)	2.884(1)	Ga(3)–S(1)	2.325(1)
La(3)–S(6)	2.895(1)		

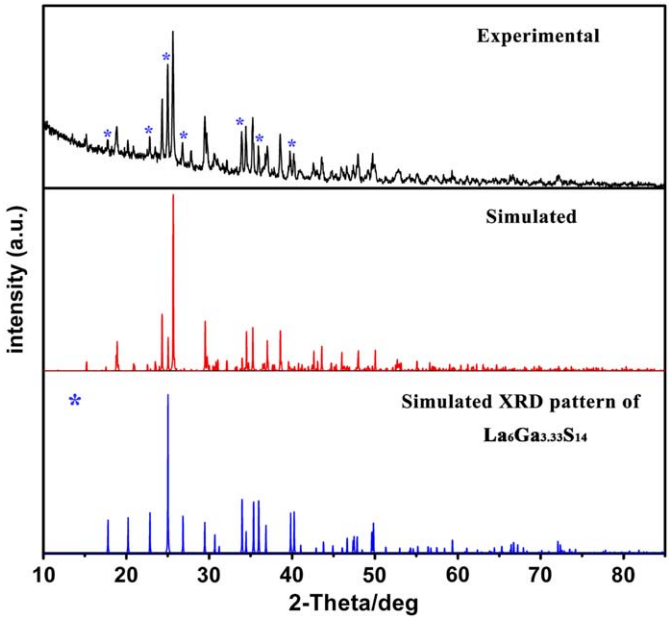

Fig. 1. Experimental and simulated XRD patterns of β-$LaGaS_3$ and the simulated XRD patterns of the byproduct $La_6Ga_{3.33}S_{14}$.

2.4. Elemental analysis

The elemental analyses of La, Ga, and S have been examined on handpicked single crystals of β-$LaGaS_3$ with the aid of a field emission scanning electron microscope (FESEM, JSM6700F) equipped with an energy dispersive X-ray spectroscope (EDX, Oxford INCA).

2.5. UV/Vis diffuse reflectance spectroscopy

The optical diffuse reflectance spectrum of the handpicked single crystals of β-$LaGaS_3$ sample was measured at room temperature using a Perkin–Elmer Lambda 900 UV–Vis spectrophotometer equipped with an integrating sphere attachment and $BaSO_4$ as a reference. The absorption spectrum was calculated from the reflection spectrum via the Kubelka–Munk function: $\alpha/S=(1-R)^2/2R$, in which α is the absorption coefficient, S is the scattering coefficient, and R is the reflectance [16].

2.6. Second harmonic generation

The SHG was measured by using the Kurtz and Perry method with a 2.05 μm Q-switch laser [17]. A sample of LGS was prepared as a reference material in an identical fashion. The SHG was measured on the powders mostly ground from the handpicked β-$LaGaS_3$ crystals plus small amount of the as-synthesized product.

2.7. Electronic structure calculations

The electronic structure calculations of α- and β- $LaGaS_3$ were performed with the highly accurate full-potential linear augmented plane wave plus local orbital (FP-LAPW+LO) method within the density-functional theory (DFT) [18–20], implemented in the WIEN2k program package [21]. The Perdew–Burke–Ernzerhof generalized gradient approximation (PBE-GGA) for the exchange-correlation potentials were used in the calculations [22]. The electronic configurations for La, Ga, S are as follows: La, $[Xe]5d^16s^2$; Ga,$[Ar]3d^{10}4s^24p^1$;s,$[Ne]3s^23p^4$. The values of the atomic radii were taken to be 2.50 au for La, 2.06 au for Ga, and 2.06 au for S. Convergence of the self-consistent iterations was performed for 20 k points inside the irreducible Brillouin zone to within 0.0001 Ry with a cutoff -7 Ry between the valence and the core states.

3. Results and discussion

3.1. Synthesis

The title compound was synthesized from the elemental mixture of La, Ga and S with the a ratio of 1:1:3 at 1100 °C. The EDX result on single crystals of β-$LaGaS_3$ confirms the presence of La, Ga and S with a molar ratio around 1:1:3. No other element, such as Si, O from the reaction container, was found in any case. The X-ray diffraction (XRD) analyses showed the coexistence of $La_6Ga_{3.33}S_{14}$, ($Ce_6Al_{3.33}S_{14}$ type, ICSD-27022) (Fig. 1). Great efforts had been made to obtain single phased β-$LaGaS_3$ powdery sample, such as elongation of the reaction time from 48 to 120 h, and decrease of the anneal temperature from 900 to 820 °C, etc. Unfortunately, the byproduct, $La_6Ga_{3.33}S_{14}$ (about 40%), was irremovable by such treatments. However, we could manually separate the different crystals by their distinguished color, β-$LaGaS_3$, light yellow, and $La_6Ga_{3.33}S_{14}$, dark brown. The UV–vis diffuse reflectance (below) is measured on the powders ground merely from the handpicked crystals of β-$LaGaS_3$.

3.2. Crystal structure

The non-centrosymmetric β-$LaGaS_3$ crystallizes in $Pna2_1$ (No.33) with a=10.405(1) Å, b=21.984(2) Å, c=6.0565(5) Å, V=1385.3(2) $Å^3$ and Z=12 (Fig. 2). It is an isomeric compound of α-$LaGaS_3$ ($P2_1/c$, No. 14) (Fig. 3) [13]. The main structural motif of β-$LaGaS_3$ is the wavy chains made of GaS_4 tetrahedra that are extending along the [100] direction and separated by La^{3+} cations (Fig. 2). Each of the three crystallographically independent Ga atoms adopts tetrahedral coordination sphere (T), and Ga1- and Ga2-centered polyhedra are interconnected through sharing S6 and S7 atoms (Fig. 4a). The Ga3-centered T3 appends to the wavy chain at T2 via S1 atoms. All Ga–S bonds range from 2.194 to 2.325 Å, which are close to the Ga–S bonds in $LiGaS_2$ (2.269–2.281 Å) [23] and $BaGa_4S_7$ (2.229–2.338 Å) [24].

Such a structure is an isomer of the known α-$LaGaS_3$ [13] (a=10.330 Å, b=12.820 Å, c=10.560 Å, γ=98.9°, and V=1381.6 $Å^3$,

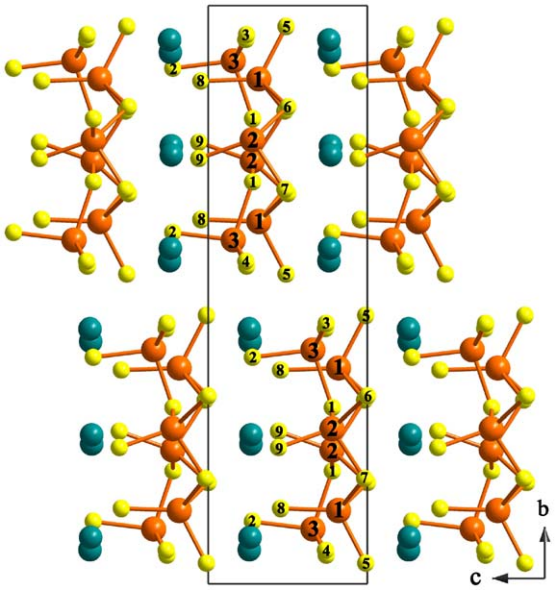

Fig. 2. Structure of β-$LaGaS_3$ viewed along the a axis: Dark cyan, La; Orange, Ga; Yellow, S. (For interpretation of the references to the color in this figure legend, the reader is referred to the web version of this article.)

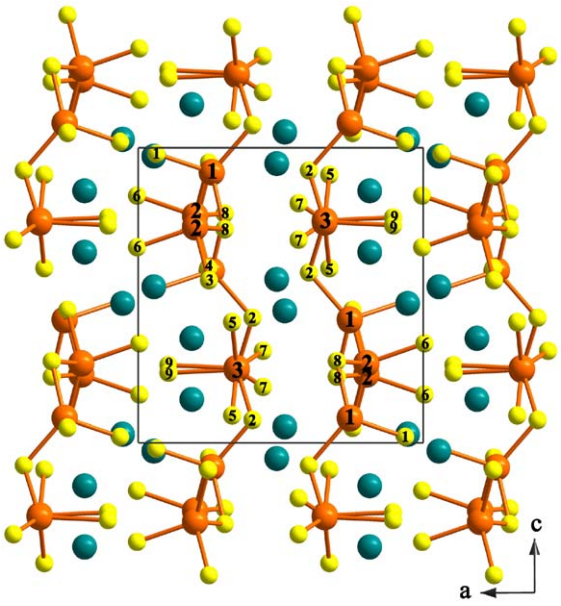

Fig. 3. Structure of α-$LaGaS_3$ viewed along the b axis: Dark cyan, La; Orange, Ga; Yellow, S. (For interpretation of the references to the color in this figure legend, the reader is referred to the web version of this article.)

monoclinic, $P2_1/c$, No. 14) (Fig. 3). Both isomeric $LaGaS_3$ compounds are chain compounds in which the chains are all made of GaS_4 tetrahedra. To simplify, if only the translation operation was under consideration, the repeating unit of each chain was a string of six GaS_4 tetrahedra as indicated in Fig. 4. There are two major differences between β- and α-$LaGaS_3$. One is the appending position of the appendant tetrahedra (T3): attaching at the middle of the side of the wave in β-$LaGaS_3$ (Fig. 4a) or at the turning point of the wave in α-$LaGaS_3$ (Fig. 4b). Another is the different bending angles: $\angle T_2–T_1–T_2 = \sim 88°$ in the former and $\sim 125°$ in the latter. Besides, the packing of the chains in β-$LaGaS_3$ is looser than that in α-$LaGaS_3$, because the density of GaS_4 tetrahedron per unit cell of β-$LaGaS_3$ is slightly smaller than that of α-$LaGaS_3$, 2.38 vs. 2.39 $g\,cm^{-3}$.

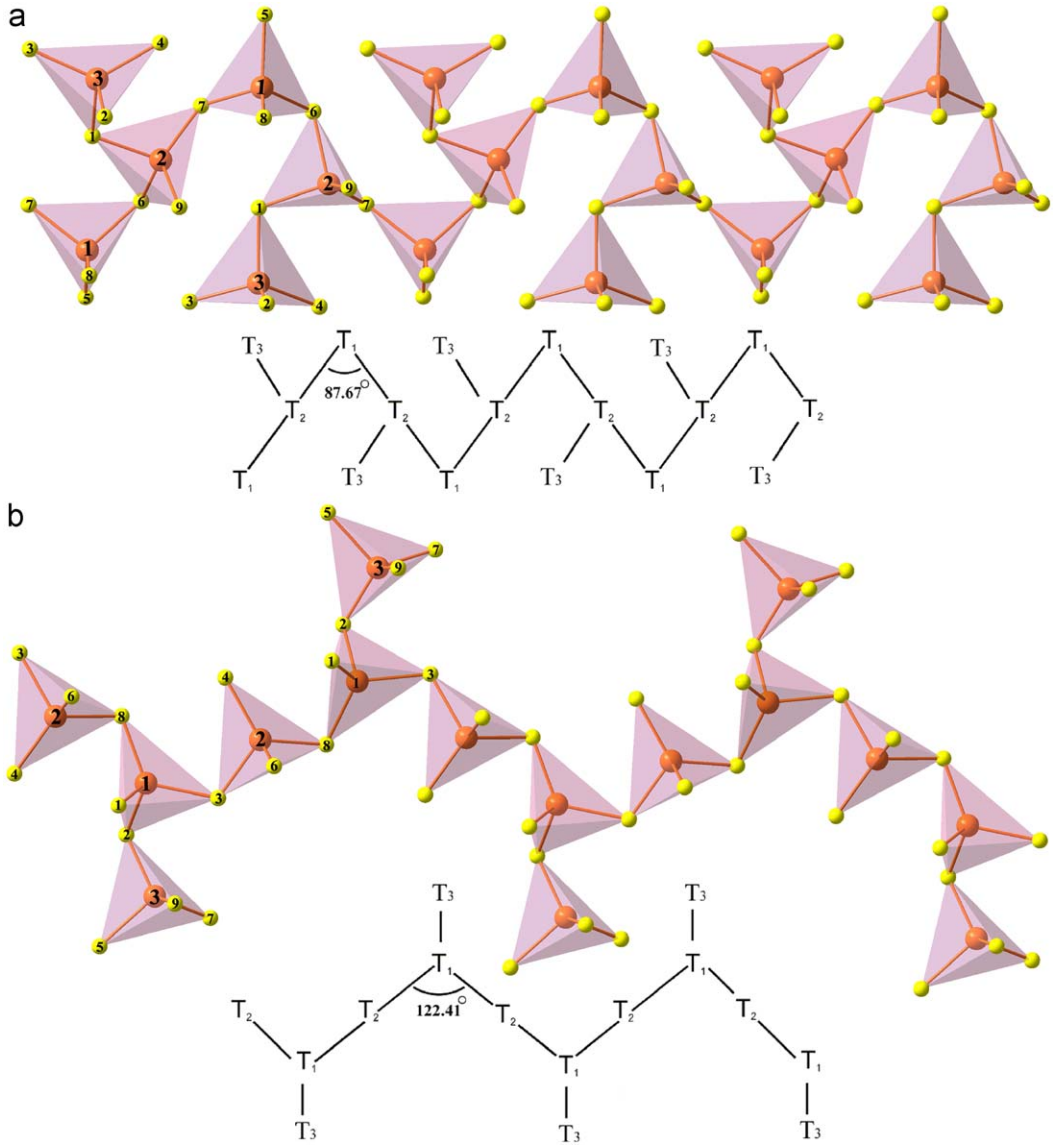

Fig. 4. Part of the wavy GaS_4 tetrahedron chain and the sketch of (a) β-$LaGaS_3$ and (b) α-$LaGaS_3$. Ga(1), Ga(2), and Ga(3) are marked as 1, 2, and 3, respectively. Orange, Ga; Yellow, S. T_1, T_2, and T_3 represent $Ga1S_4$, $Ga2S_4$, and $Ga3S_4$, respectively. (For interpretation of the references to the color in this figure legend, the reader is referred to the web version of this article.)

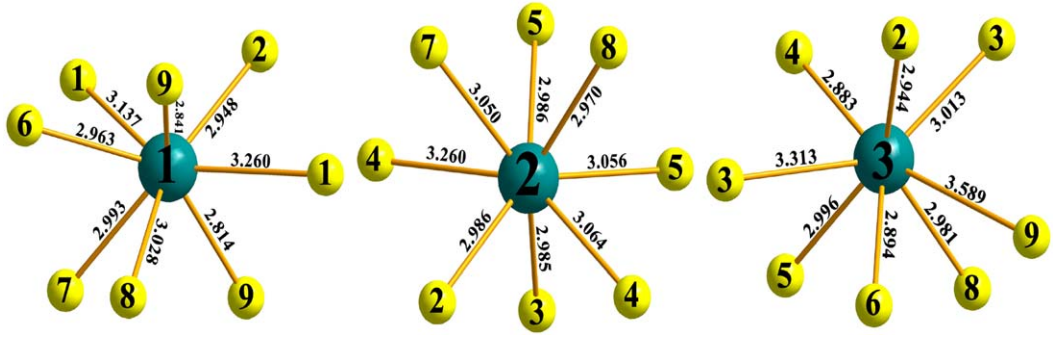

Fig. 5. The local coordination environment of La atom. Dark cyan, La; Yellow, S. (For interpretation of the references to the color in this figure legend, the reader is referred to the web version of this article.)

As shown in Fig. 5, each La atom is bonded with eight neighboring S atoms that are best described as a distorted bicapped trigonal prism, a coordination polyhedron often found in rare-earth chalcogenides. The La–S distances are between 2.814 and 3.31 Å, which are comparable to 2.93 Å in γ-La_2S_3 [25], 2.91 Å in orthorhombic α-La_2S_3 [26], and 2.780 Å–3.393 Å in $La_7Sb_9S_{24}$ [27].

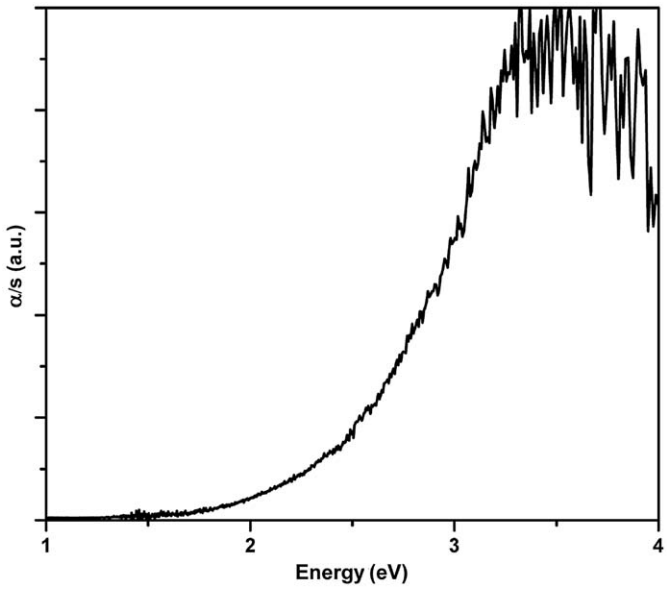

Fig. 6. UV–vis diffuse reflectance of β-$LaGaS_3$.

3.3. Optical band gap

The band gap of β-$LaGaS_3$ is measured to be ~2.5 eV (measured on the powders ground from the handpicked single crystals, Fig. 6). Such a value is in agreement with the light yellow color of β-$LaGaS_3$ and suggests the semiconductor behavior. The band gap of β-$LaGaS_3$ is also comparable to the reported value for some other related compounds, such as $LiGaS_2$ (3.87 eV) [23], $AgGaS_2$ (2.64 eV) [28] and α-La_2S_3 (1.7–2 eV) [29].

According to the theoretical study on the NLO properties of the *X*GS (*X*=Li, La, Ba) family with the ab initio method [30], GaS_4 tetrahedral group provides the main contribution to the overall NLO coefficients. The non-centrosymmetric β-$LaGaS_3$ is also constructed by similar GaS_4 tetrahedron and should also exhibit NLO response. We have therefore primarily measured the second-harmonic signal of the powders mostly ground from the handpicked β-$LaGaS_3$ crystals plus small amount of the as-synthesized powders. The signal is very weak. We consider the coexistence of the byproduct may have some negative influence. Continuous synthesis efforts to obtain single phased β-$LaGaS_3$ are on going.

3.4. Electronic structure

In the early 1980s, Julien-Pouzol et al. had reported the synthesis and structure of α-$LaGaS_3$ [13], but the calculation of the electronic structures and the optical properties had not been studied. Here, we report the calculations on the electronic structure and optical properties of both α- and β-$LaGaS_3$.

The total and partial densities of states for α- and β-$LaGaS_3$ are presented in Fig. 7. The conduction bands (CB) of both compounds are composed of La 5*d* and Ga 4*s* orbitals, whereas the valence bands (VB) are constructed by dominating S 3*p* bands and minor contributions from Ga 4*p* and La 5*d* orbitals. The DOS curves (Fig. 7) indicate that the maxima of HOVB of both compounds are composed of S 3*p* bands. The enlarged pictures in Fig. 8 show that the minima of LUCB of both compounds are composed of Ga 4 s states which locate at ~2.2 eV in β-$LaGaS_3$ and ~1.9 eV in α-$LaGaS_3$. Thus, the band gaps of these two $LaGaS_3$ are determined by the energies of S 3*p* and Ga 4*s* bands.

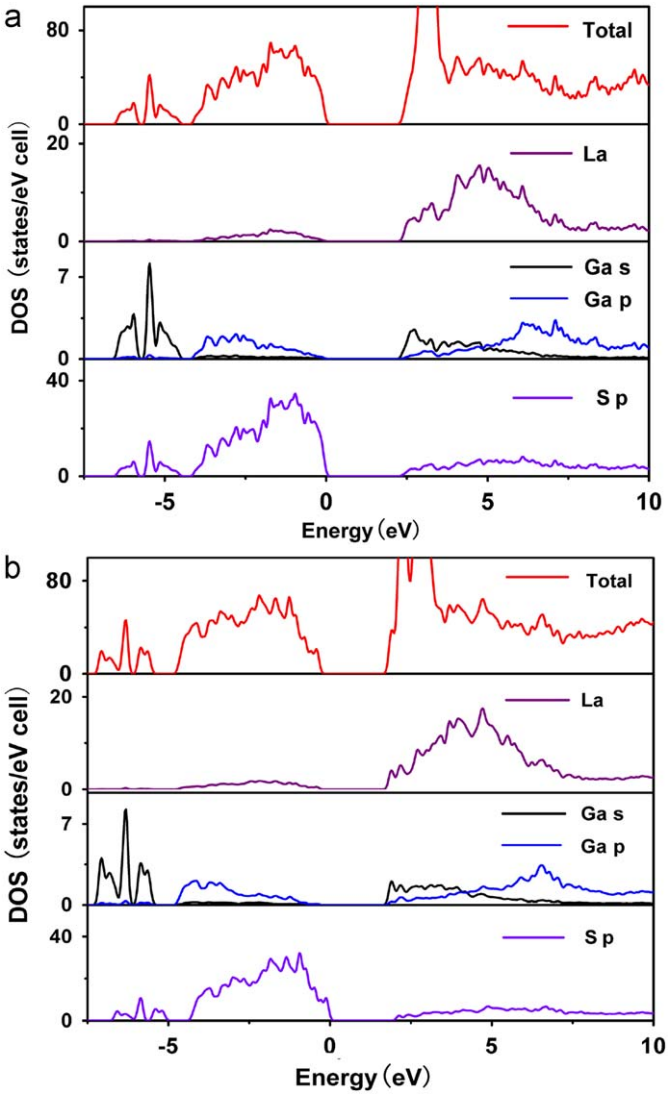

Fig. 7. Total and partial density of states of (a) β-$LaGaS_3$; (b) α-$LaGaS_3$.

Similar as binary La_2S_3 and Ga_2S_3, β-$LaGaS_3$ is an electron-precise intrinsic semiconductor. As shown in Fig. 9, the highest energy of VB of β-$LaGaS_3$ is located at G point whereas the lowest of CB is at Z point, thus β-$LaGaS_3$ is an indirect band-gap compound. Differently, for compound α-$LaGaS_3$, both the top of the VB and the bottom of the CB locate at G-point, indicating a direct band gap semiconductor characteristic. The HOVB (highest occupied VB) and LUCB (lowest unoccupied CB) of these two compounds show obvious differences. For example, the bands along Z–G (the extending direction of $(GaS_3)_n$ chains) around the Fermi level are flat for α-$LaGaS_3$, but fluctuant for β-$LaGaS_3$. Such fluctuation of β-$LaGaS_3$ is understandable considering its crystal structure motif shown in Fig. 4. That is to say, the density of a single GaS_4 tetrahedral chain in β-$LaGaS_3$ was greater than that in α-$LaGaS_3$. As a result, the interaction between GaS_4 tetrahedra in β-$LaGaS_3$ should be stronger than that in α-$LaGaS_3$, thus, the bands are more fluctuant in β-$LaGaS_3$. The computational indirect band gap of β-$LaGaS_3$ is about 2.3 eV, slightly smaller than the experimental value of 2.5 eV.

Moreover, we have also calculated the formation heat for both compounds. The result shows that their stabilities are almost the same. The formation heat of α-$LaGaS_3$ is only 0.21 kJ/mol higher than that of β-$LaGaS_3$.

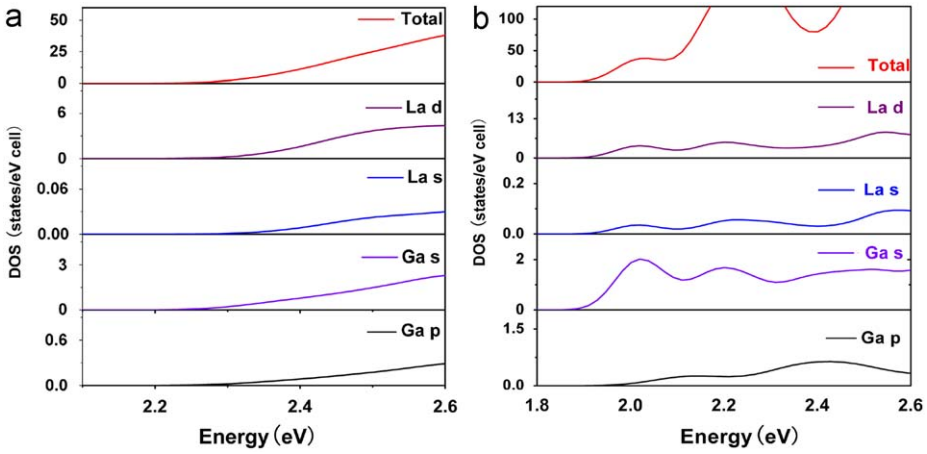

Fig. 8. The compositions of the minima of LUCB: (a) β-$LaGaS_3$ from 2.1–2.6 eV; (b) α-$LaGaS_3$ from 1.8–2.6 eV.

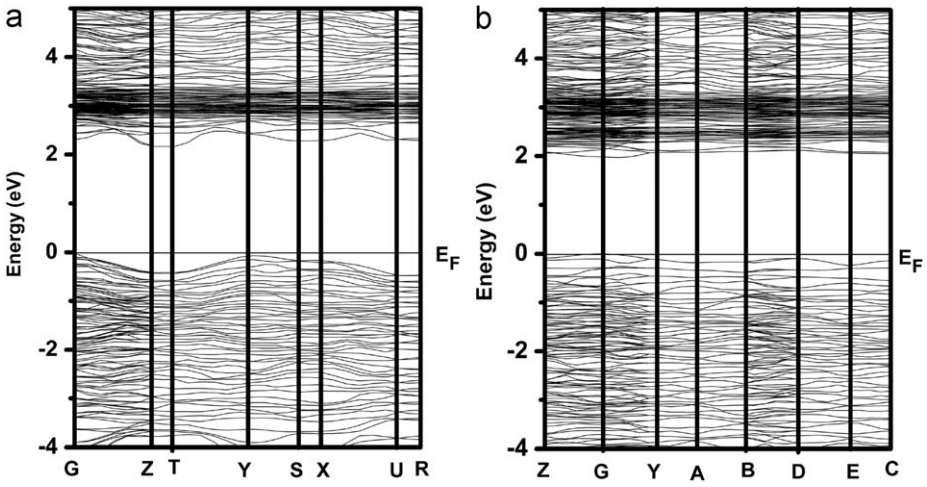

Fig. 9. Band structures of (a) β-$LaGaS_3$; (b) α-$LaGaS_3$.

3.5. Optical properties

The optical properties of matter can be described by the means of the dielectric function $\varepsilon(\omega)$ [31]. The real and imaginary parts of $\varepsilon(\omega)$ are often referred to as $\varepsilon_1(\omega)$ and $\varepsilon_2(\omega)$, respectively. The imaginary part can be calculated from the momentum matrix elements between the occupied and unoccupied wave functions and given by the Kubo–Greenwood formula. The real part is deduced from the imaginary value via the Kramers–Kronig relation [32].

The real part of the dielectric function $\varepsilon_1(\omega)$ and the imaginary part $\varepsilon_2(\omega)$ of both β- and α-$LaGaS_3$ are plotted in the energy range of 0.0–22.5 eV as shown in SFigs. 1 and 2. The differences between the dispersion of the function ε_{xx}, ε_{yy}, ε_{zz} are correlated to the anisotropy of the crystal. The imaginary part $\varepsilon_2(\omega)$ of the dielectric function is associated with the interband transitions, where the intraband transitions are ignored because the intraband transitions are considered to be important only in metallic materials [32]. In β-, and α-$LaGaS_3$, the main peaks of imaginary part $\varepsilon_2(\omega)$ locate around 5.60 and 5.40 eV, respectively, which can be attributed to the interband transitions from S 3*p* VB to Ga 4*s* CB. One may note that the general shapes of ε_2 curves for both compounds are rather similar, which indicates the same frequency regions, where the $\varepsilon_2(\omega)$ functions are enhanced or decreased in one polarization or the other. This is because of the similarities in their underlying band structures. Our calculated absorption edges of the two compounds are 2.37 eV (β-$LaGaS_3$) and 1.90 eV (α-$LaGaS_3$), respectively, corresponding to their band gaps. In the aspect of the real part $\varepsilon_1(\omega)$, the most important quantity is the zero frequency limit $\varepsilon_1(0)$, which is the electronic part of the static dielectric constant. Our calculated static dielectric constants $\varepsilon_1(0)$ for both compounds are listed in Table 3.

Table 3
Static dielectric constants ε_1 (0) of β-$LaGaS_3$ and α-$LaGaS_3$.

	β-$LaGaS_3$	α-$LaGaS_3$
ε_{1xx}	7.499	7.179
ε_{1yy}	7.170	7.554
ε_{1zz}	7.448	7.471
$\overline{\varepsilon}$	7.372	7.401

SFigs. 3–5 show the calculated results on the energy dependence of the refractive index $n(\omega)$, absorption coefficient $I(\omega)$ and reflectivity $R(\omega)$, respectively. Taking β-$LaGaS_3$ for example, the function $n(\omega)$ appears its peak value around 3.5 eV and decreases rapidly in the region from 5.4 to 16.0 eV, corresponding mainly to the higher values of $R(\omega)$ in this range.

The absorption coefficient $I(\omega)$ is very large (about $10^6\,cm^{-1}$), which may be caused by the free carrier adsorptions in semiconductors [33]. Similar phenomena of the large absorption can also be found in other sulfides, such as $Ga(In)_2S_3$ [34], $LiInS_2$ [35]. The light propagation process in a semiconductor can generate conduction current, which converts part of the light energy into the joule heat. The absorption spectra explain why the color of β-$LaGaS_3$ is light yellow because the absorption starts around 2.45 eV, which lies in the high-frequency region of the visible spectrum, such as green light, whereas, low frequencies are not absorbed and they will therefore dominate the transmitted light. The variation of reflectance as a function of photon frequency is displayed in Fig. S5. The dynamic reflectance corresponds to the ratio of the intensities of the incident and reflected electric fields. In the low energy regime, the reflectivity increases slowly from 0.2 to 0.4. The small value of the reflectance ensures its applications as transparent coatings in IR to visible and UV light regime. The optical properties of α-, and β-$LaGaS_3$ are very similar, because of their similar structure and electronic structure.

4. Conclusion

In summary, a new ternary non-centrosymmetric β-type $LaGaS_3$ compound has been successfully synthesized. β-$LaGaS_3$ is an isomer of the monoclinic α-$LaGaS_3$ reported in 1982 [13], and its main structural motif is the GaS_4 tetrahedron chains extending along [100] direction that are separated by La^{3+} cations. Electronic structure calculations on both β- and α-$LaGaS_3$ by WIEN2k indicate that β-type is an indirect and α-type is a direct band gap semiconductor. The dispersions of the bands around the Fermi level of these two compounds are different that are thought to be caused by the different packing densities of the GaS_4 tetrahedron chains in each compound. The calculated optical properties of two compounds are similar, and the calculated band gap of β-$LaGaS_3$ agrees well with the experimental measurement $E_{g(cal)}$=2.3 vs. $E_{g(cal)}$= ~2.5 eV. The calculated absorption spectrum of β-$LaGaS_3$ explains well the color of this compound. Besides, the weak NLO response of β-$LaGaS_3$ has been detected.

Acknowledgments

This research was supported by the National Natural Science Foundation of China under Projects (20773130, 20733003, 20821061), 973 Program (2009CB939801), the "Key Project from CAS" (KJCX2-YW-H20, CXJJ-219), and the "Key Project from FIRSM" (SZD08002).

Appendix A. Supplementary material

Supplementary data associated with this article can be found in the online version at doi:10.1016/j.jssc.2009.11.030.

References

[1] G.D. Boyd, E. Buehler, F.G. Storz, J. Wernick, IEEE J. Quantum Electron. 8 (1972) 419–426.
[2] C.T. Chen, L. Bai, Z.Z. Wang, R.K. Li, J. Cryst. Growth. 292 (2006) 169–178.
[3] Q.C. Zhang, I. Chung, J.I. Jang, M.G. Kanatzidis, Chem. Mater. 21 (2009) 12–14.
[4] Q.C. Zhang, I. Chung, J.I. Jang, M.G. Kanatzidis, J. Am. Chem. Soc. 131 (2009) 9896–9897.
[5] S. Banerjee, C.D. Malliakas, J.I. Jang, J.B. Ketterson, M.G. Kanatzidis, J. Am. Chem. Soc. 130 (2008) 12270–12272.
[6] I. Chung, J.H. Song, J.I. Jang, A.J. Freeman, J.B. Ketterson, M.G. Kanatzidis, J. Am. Chem. Soc. 131 (2009) 2647–2656.
[7] J. Kim, T. Hughbanks, Inorg. Chem. 39 (2000) 3092–3097.
[8] L.H. Li, J.Q. Li, L.M. Wu, J. Solid State Chem. 181 (2008) 2462–2468.
[9] J.L. Adam, Chem. Rev. 102 (2002) 2461–2476.
[10] D.W. Hewak, R.C. Moore, T. Schweizer, J. Wang, B. Samson, W.S. Brocklesby, D.N. Payne, E.J. Tarbox, Electron. Lett. 32 (1996) 384–385.
[11] A.K. Mairaj, R.J. Curry, D.W. Hewak, Electron. Lett. 40 (2004) 421–422.
[12] T. Schweizer, D.W. Hewak, D.N. Payne, T. Jensen, G. Huber, Electron. Lett. 32 (1996) 666–667.
[13] M. Julien-Pouzol, S. Jaulmes, C. Dagron, Acta Crystallogr. Sect. B 38 (1982) 1566–1568.
[14] D. de Saint-Giniez, P. Laruelle, J. Flahaut, Compt. Rend C 267 (1968) 1029–1032.
[15] G.M. Sheldrick, SHELXTL, Crystallographic Software Package, SHELXTL, Version 5.1, Bruker-AXS, Madison, WI, 1998.
[16] G. Kortüm, Reflectance Spectroscopy, Springer, New York, 1969.
[17] S.K. Kurtz, T.T. Perry, J. Appl. Phys. 39 (1968) 3798–3813.
[18] R. Yu, H. Krakauer, D. Singh, Phys. Rev. B. 43 (1991) 6411–6422.
[19] E. Wimmer, H. Krakauer, M. Weinert, A.J. Freeman, Phys. Rev. B. 24 (1981) 864–866.
[20] L.F. Mattheiss, D.R. Hamann, Phys. Rev. B. 33 (1986) 823–840.
[21] P. Blaha, K. Schwarz, G.K.H. Madsen, D. Kvasnicka, J. Luitz, WIEN2k, An Augmented Plane Wave Plus Local Orbitals Program for Calculating Crystal Properties, Vienna University of Technology, 2001.
[22] [a] K.P. Ong, K. Bai, P. Blaha, P. Wu, Chem. Mater. 19 (2007) 634–640;
[b] Y. Hinuma, Y.S. Meng, K.S. Kang, G. Ceder, Chem. Mater. 19 (2007) 1790–1800.
[23] A. Yelisseyev, S. Lobanov, A. Titov, V. Petrov, J.J. Zondy, P. Krinitsin, A. Merkulov, V. Vedenyapin, J. Smirnova, L. Isaenko, Cryst. Res. Technol. 38 (2003) 379–387.
[24] X. Lin, G. Zhang, N. Ye, Cryst. Growth Des. 9 (2009) 1186–1189.
[25] R. Mauricot, P. Gressier, M. Evain, R. Brec, J. Alloys Compd. 223 (1995) 130–138.
[26] A.W. Sleight, C.T. Prewitt, Inorg. Chem. 7 (1968) 2282–2288.
[27] A. Assoud, K.M. Kleinke, H. Kleinke, Chem. Mater. 18 (2006) 1041–1046.
[28] S. Laksari, A. Chahed, N. Abbouni, O. Benhelal, B. Abbar, Comput. Mater. Sci. 38 (2006) 223–230.
[29] K.A. Gschneidner, B.J. Beaudry, T. Takeshita, S.S. Eucker, S.M.A. Taher, J.C. Ho, J.B. Gruber, Phys. Rev. B. 24 (1981) 7187–7193.
[30] B. Lei, Z.S. Lin, Z.Z. Wang, C.T. Chen, J. Appl. Phys. 103 (2008) 083111.
[31] P. Ravindran, A. Delin, R. Ahuja, B. Johansson, S. Auluck, J.M. Wills, O. Eriksson, Phys. Rev. B. 56 (1997) 6851–6861.
[32] H. Haiying, O. Roberto, A.B. Miguel, P. Ravindra, A. Emilie, B. Isabelle, R. Michel, Phys. Rev. B. 74 (2006) 195123.
[33] D. Vanmaekelbergh, L. van Pieterson, Phys. Rev. Lett. 80 (1998) 821.
[34] C. Sanz, C. Guillen, M.T. Gutierrez, J. Phys. D: Appl. Phys. 40 (2008) 235103.
[35] K. Kuriyama, T. Kato, A. Takahashi, Phys. Rev. B 46 (1992) 15518.